Bioorganic Chemistry 89 (2019) 102985

Contents lists available at ScienceDirect

Bioorganic Chemistry

journal homepage: www.elsevier.com/locate/bioorg

Synthesis and *in vitro* anticancer evaluation of some fused indazoles, quinazolines and quinolines as potential EGFR inhibitors

Esraa A. Abdelsalam[a,*], Wafaa A. Zaghary[a], Kamilia M. Amin[b], Nageh A. Abou Taleb[a], Amal A.I. Mekawey[c], Wagdy M. Eldehna[d], Hatem A. Abdel-Aziz[e], Sherif F. Hammad[a,*]

[a] Pharmaceutical Chemistry Department, Faculty of Pharmacy, Helwan University, P.O. Box 11795, Ain Helwan, Cairo, Egypt
[b] Department of Pharmaceutical Chemistry, Faculty of Pharmacy, Cairo University, Kasr El-Aini Street, P.O. Box 11562, Cairo, Egypt
[c] Regional Center of Mycology and Biotechnology, Al-Azhar University, Cairo, Egypt
[d] Department of Pharmaceutical Chemistry, Faculty of Pharmacy, Kafrelsheikh University, P.O. Box 33516, Kafrelsheikh, Egypt
[e] Department of Applied Organic Chemistry, National Research Centre, P.O. Box 12622, Dokki, Giza, Egypt

ARTICLE INFO

Keywords:
Anticancer
EGFR inhibitors
Molecular docking
Benzo[*g*]indazole
Benzo[*h*]quinazoline
Benzo[*h*]quinoline

ABSTRACT

derivatives of benzo[*g*]indazole **5a, b**, benzo[*h*]quinazoline **7**, **12a-c**, **13a-c** and **15a-c** and benzo[*h*]quinoline **17a-c** and **19a-c** were synthesized from 6-methoxy-3,4-dihydronaphthalen-1(2*H*)-one (**1**). Anticancer activity of all the synthesized compounds was evaluated against four cancerous cell lines; HepG2, MCF-7, HCT116 and Caco-2. MCF-7 cells emerged as the most sensitive cell line against the target compounds. All the examined compounds, except **5a** and **5b**, displayed potent to moderate anticancer activity against MCF-7 cells with an IC_{50} values ranging from 7.21 to 21.55 μM. In particular, compounds **15c** and **19b** emerged as the most potent derivatives against EGFR-expressing MCF-7 cells with IC_{50} values = 7.70 ± 0.39 and 7.21 ± 0.43 μM, respectively. Additionally, both compounds did not display any significant cytotoxicity towards normal BHK-21 fibroblast cells (IC_{50} value > 200 μM), thereby providing a good safety profile as anticancer agents. Furthermore, compounds **15c** and **19b** displayed potent inhibitory activity towards EGFR in the sub-micromolar range (IC_{50} = 0.13 ± 0.01 and 0.14 ± 0.01 μM, respectively), compared to that of Erlotinib (IC_{50} = 0.11 ± 0.01 μM). Docking studies for **15c** and **19b** into EGFR active site was carried out to explore their potential binding modes. Therefore, compounds **15c** and **19b** can be considered as interesting candidates for further development of more potent anticancer agents.

1. Introduction

Cancer remains as a major health problem and a life-threatening disease. It is considered the second leading cause of mortality, after cardiovascular diseases, accounting for about 14.6% of deaths globally [1]. Among women, breast cancer has stood out as the most frequently diagnosed cancer and the second leading cause of cancer-related deaths in women [2]. The conventional chemotherapy displays a pivotal role in the treatment of various types of cancers, nevertheless, there are numerous challenges [3], of which the poor selectivity that causes undesired side effects on normal cells, stands out as the major one [4]. Multiple drug resistance (MDR) [5,6], the ability of neoplastic cells to survive under anaerobic conditions [7] and the incorporation of multiple enzymes at different stages of cancer development [8] are among the other cancer challenges. These entire challenges make the development of more selective, safer and effective therapies for human malignancies an urgent and critical demand.

Epidermal growth factor receptor (EGFR), a receptor tyrosine kinase, displays a vital role regarding the regulation of numerous cellular functions such as cell proliferation, survival, differentiation and migration [9]. EGFR mediates intracellular signaling (intrinsic intracellular protein-tyrosine kinase activity) in response to various extracellular stimuli (endogenous ligand, like epidermal growth factor (EGF) and transforming growth factor α (TGFα)), leading to DNA synthesis and cell growth [10,11]. Mutations which cause EGFR overexpression and activation are associated with wide variety of cancer types as breast cancer, colorectal carcinoma, non-small cell lung cancer, pancreatic cancer and hepatocellular carcinoma [12]. Accordingly, interruption of the signaling pathway of EGFR, either extracellularly by blocking the binding site of EGFR or intracellularly by inhibiting the tyrosine kinase activity, is important in cancer prevention and treatment [13,14]. It has been established that EGFR is one of the most

* Corresponding authors.
E-mail addresses: esraa.amgad@pharm.helwan.edu.eg (E.A. Abdelsalam), sherif.hammad@pbichem.com (S.F. Hammad).

https://doi.org/10.1016/j.bioorg.2019.102985
Received 16 December 2018; Received in revised form 11 April 2019; Accepted 14 May 2019
Available online 15 May 2019
0045-2068/

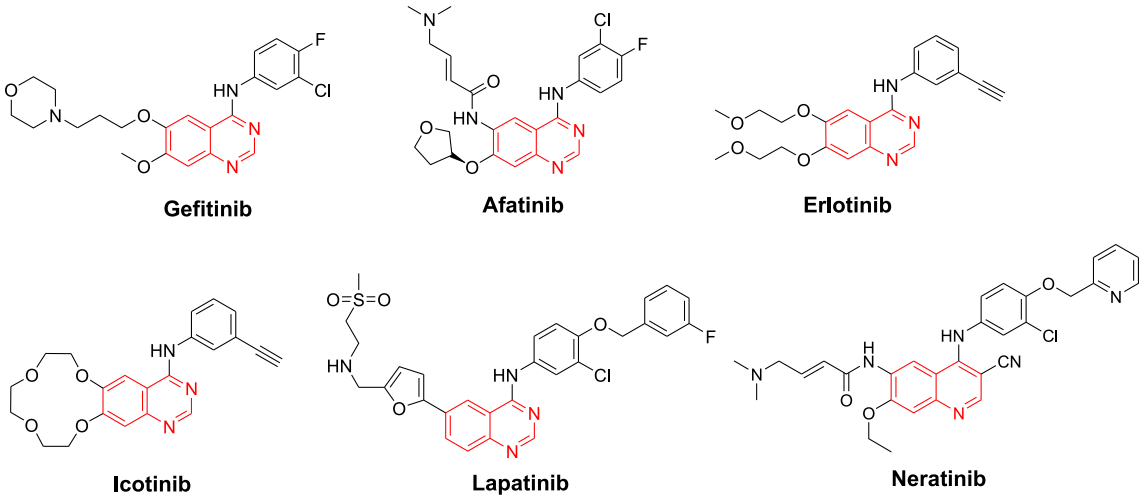

Fig. 1. Some clinically approved EGFR-TK inhibitors based on quinazoline and quinoline scaffolds.

important targets for development of novel breast cancer therapeutics [15–17].

In the current medical era, quinazoline is one of the most important heterocyclic scaffolds that emerged as a promising privileged scaffold in cancer drug discovery [18–20]. Interestingly, there are many clinically approved quinazoline-based anticancer drugs with potent EGFR-TK inhibitory activity such as Gefitinib (Iressa®) [21], Afatinib (Gilotrif®) [22], Erlotinib (Tarceva®) [23], Icotinib (Conmana®) [24] and Lapatinib (Tykerb®) (Fig. 1) [25].

Furthermore, quinoline is an interesting fused heterocyclic scaffold present in a variety of FDA-approved marketed anticancer drugs [26] such as; Neratinib (Nerlynx®) [27] which is EGFR-TK inhibitor (Fig. 1), Cabozantinib (Cabometyx®) [28], Bosutinib (Bosulif®) [29] and Lenvatinib (Lenvima®) [30], which are protein kinase inhibitors (Fig. 2).

Moreover, indazole is a well-known fused heterocyclic nucleus possessing interesting biological activities [31–33]. Indazole emerged as an attractive scaffold to develop new anticancer agents [34]. The FDA approved drug; Pazopanib (Votrient®) is an example of indazole based multi-targeted receptor tyrosine kinase inhibitor [35] (Fig. 2).

In the light of the previous facts, herein we reported the synthesis of different sets of benzo[*g*]indazole **5a, b**, benzo[*h*]quinazoline **7**, **12a-c**, **13a-c** and **15a-c**, and benzo[*h*]quinoline **17a-c** and **19a-c** derivatives. All the previously prepared and novel derivatives were evaluated for their potential anticancer activity against four cancer cell lines; liver carcinoma cell line (HepG2), breast carcinoma cell line (MCF-7), colon carcinoma cell line (HCT116) and colon carcinoma cell line (Caco-2). Furthermore, the most potent counterparts in this study will be assayed for their potential inhibitory activity towards EGFR. Also, molecular docking study was performed to explore the binding mode and possible interactions with EGFR active site.

2. Results and discussion

2.1. Chemistry

The synthetic pathways adopted for the preparation of the intermediates and the target fused indazoles, quinazolines and quinolines were depicted in Schemes 1–3. In Scheme 1, 6-methoxy-3,4-dihydronaphthalen-1(2*H*)-one (**1**) was utilized in the synthesis of the 2-acetyl-6-methoxy-3,4-dihydronaphthalen-1(2*H*)-one (**3**) through its reaction with ethyl acetate in sodium ethoxide (Scheme 1). The keto-enol tautomeric structure of compound **3** was established on the basis of its

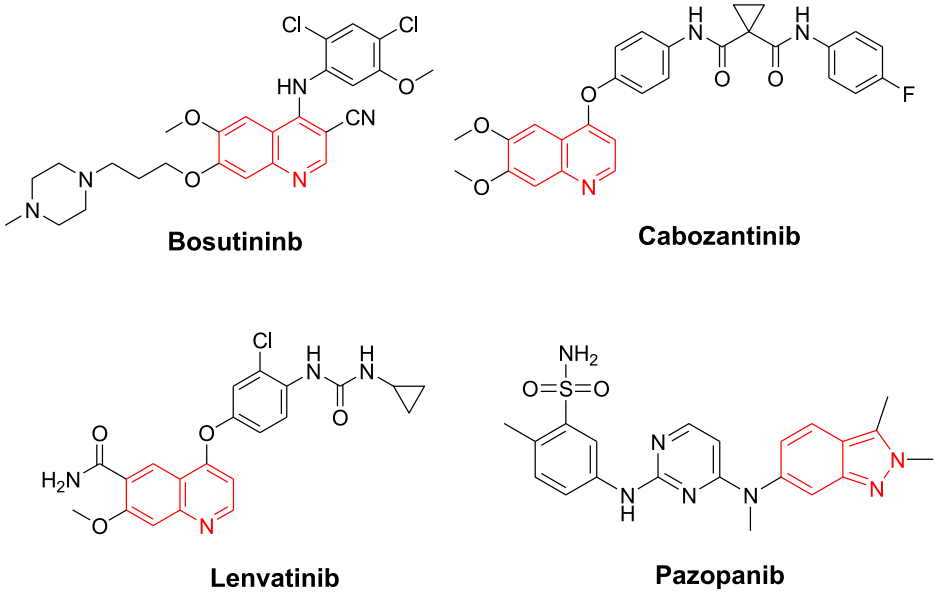

Fig. 2. Some clinically approved protein kinase inhibitors based on quinoline and indazole scaffolds.

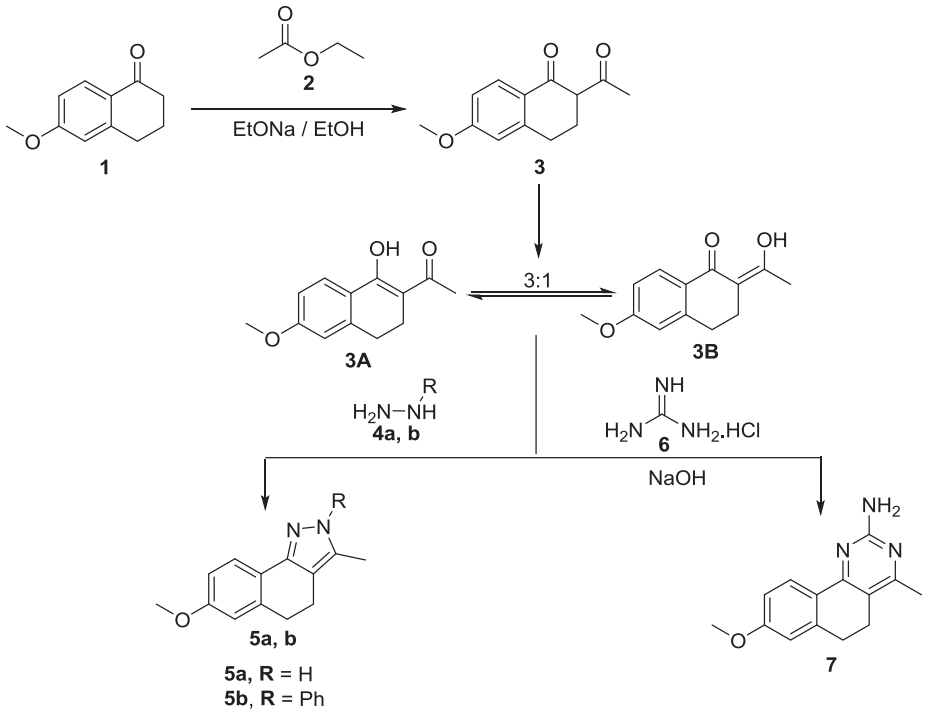

Scheme 1. Synthesis of fused indazoles **5a, b** and fused quinazoline **7**.

NMR and IR spectra. The ^{1}H NMR spectrum revealed the absence of the signal of the aliphatic hydrogen at C-2 in naphthalene moiety of 1,3-diketone structure of **3** along with the appearance of D_2O exchangeable signal of enolic OH at δ 16.57 ppm. In addition, the ^{1}H NMR spectrum revealed the presence of two sets of signals in 3:1 proportions due to the existing of compound **3** in two keto-enol tautomeric structures,

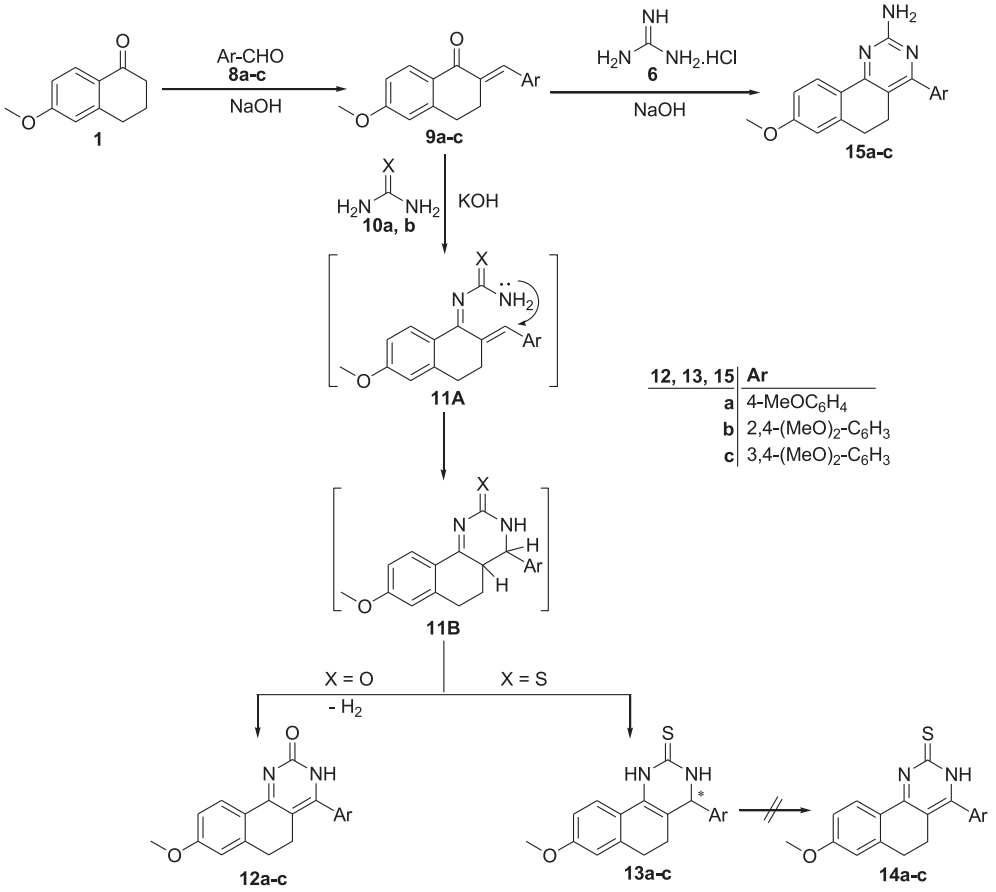

Scheme 2. Synthesis of benzo[*h*]quinazolines **12a-c**, **13a-c** and **15a-c**.

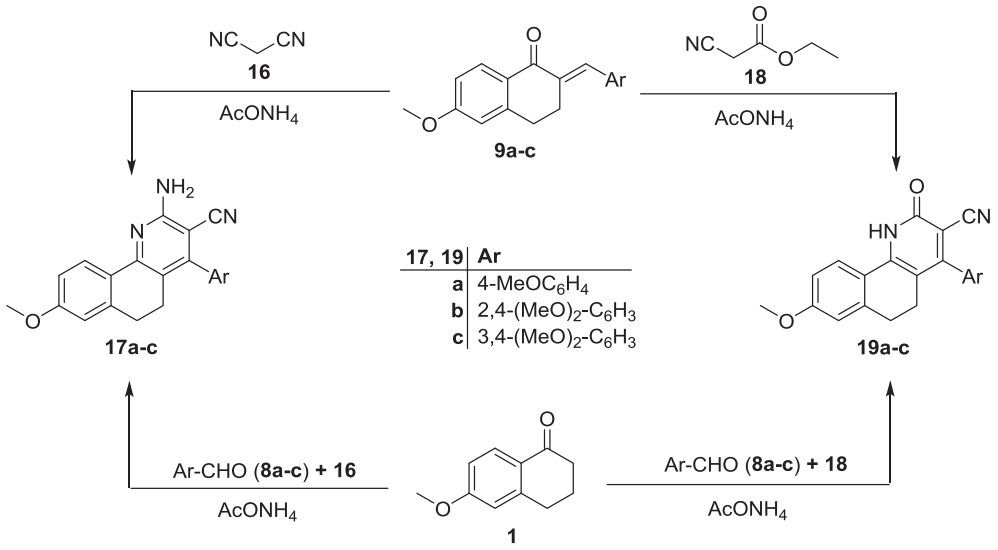

Scheme 3. Synthesis of benzo[*h*]quinolines **17a-c** and **19a-c**.

R−C(OH)═CR′−CO−Me (**3A**) and R−CO−CR′═C(OH)−Me (**3B**) in 3:1 proportions. Also, the ^{13}C NMR spectrum of compound **3** showed the signal of naphthalene C-2 (SP^2 carbon) at δ 104.7 ppm, due to keto-enol tautomeric structure for **3**, instead of the SP^3 C-2 in 1,3-diketonic structure of **3**.

Next, reaction of 2-acetyl-6-methoxy-3,4-dihydronaphthalen-1(2*H*)-one (**3**) with hydrazine hydrate (**4a**) or phenyl hydrazine (**4b**) gave the corresponding indazoles **5a**, **b**, respectively. Furthermore, treatment of compound (**4**) with guanidine hydrochloride (**6**) in refluxing ethanol, in the presence of potassium hydroxide, yielded the corresponding 8-methoxy-4-methyl-5,6-dihydrobenzo[*h*]quinazolin-2-amine (**7**) (Scheme 1).

The structures of the indazoles **5a, b** and quinazoline **7** were established on the basis of their spectral data. Their ^{1}H NMR spectra showed the singlet signals of methyl and methoxy groups at δ range 2.16–2.26 and 3.72–3.81 ppm, respectively, besides, two multiplet signals of the two methylene protons in δ range 2.55–2.71 and 2.81–2.93 ppm, respectively. While the tautomeric NH of indazole **5a** appeared as two D_2O-exchangeable singlet signals at 12.19 and 12.64 ppm, protons of the NH_2 group of quinazoline **7** appeared as a D_2O-exchangeable singlet signal at δ 6.20 ppm. Furthermore, the mass spectrum of **7** showed a peak corresponding to its molecular ion at *m/z* = 241.26 [M^+].

On the other hand, the reaction of compound (**1**) with aldehydes **8a-c** in the presence of sodium hydroxide afforded the corresponding 6-methoxy-2-(arylidene)-3,4-dihydronaphthalen-1(2*H*)-ones **9a-c**, respectively (Scheme 2). The structures of these products were established on the basis of their spectral data. For example, their ^{1}H NMR spectra exhibited the singlet signal of ═CH− proton in the region δ 7.63–7.75 ppm.

Treatment of **9a-c** with urea (**10a**) or thiourea (**10b**) in refluxing ethanol, in the presence of potassium hydroxide, afforded dihydrobenzoquinazolines **12a-c** and tetrahydrobenzoquinazolines **13a-c**, respectively (Scheme 2), in the light of their NMR spectra. ^{1}H NMR spectrum of **12b** revealed the appearance of the D_2O exchangeable signal of NH around δ 11.50 ppm. The ^{1}H NMR spectra of tetrahydrobenzoquinazolines **13a-c** showed the singlet signal of the aliphatic proton of the *chiral* C4 in the region δ 4.86–5.20 ppm in addition to the appearance of two D_2O exchangeable singlet signals of 2 NH around δ 8.60–8.95 and 9.54–9.64 ppm, respectively. ^{13}C NMR spectra of tetrahydrobenzoquinazolines **13a, c** showed the signal of the SP^3 carbon (C4) of the dihydropyrimidine ring of **13a, c** around δ 58 ppm. Interestingly, ^{1}H NMR spectra of tetrahydrobenzoquinazolines **13a-c** represented four different signals, each signal integrates to one proton of aliphatic protons of C5 and C6 (−CH_2−CH_2−). The latter findings attributed to the asymmetrical electronic environmental around the chiral C4 in dihydropyrimidine moiety. Compounds **12a-c** and **13a-c** are assumed to be formed via the initial condensation of urea (**10a**) or thiourea (**10b**), respectively, to give the intermediate **11A**. The subsequent intramolecular cyclization of **11A** through *Michael* type addition of the terminal NH_2 group to the *exo*-cyclic double bond gave the intermediate **11B**. In case of urea (**10a**), oxidation of **11B** *via* elimination of a hydrogen molecule yielded the final isolated dihydrobenzoquinazolines **12a-c** whereas in case of thiourea (**10b**), the intermediate **11B** is converted to its isolable stable tautomer tetrahydrobenzoquinazolines **13a-c** (Scheme 2). In addition, benzo[*h*]quinazolines **15a-c** were prepared by the same method used for the synthesis of compound **7** by using arylidenes **9a-c** instead of compound **3** (Scheme 2). The amino group of **15a-c** was represented by absorption bands in the region 3416–3477 and 3297–3309 cm^{-1} in their IR spectra and as D_2O exchangeable singlet signal in the region δ 6.32–6.37 *ppm* in their ^{1}H NMR spectra, respectively.

Furthermore, the reaction of 6-methoxy-2-(arylidene)-3,4-dihydronaphthalen-1(2*H*)-ones **9a-c** with malononitrile (**16**) or ethyl cyanoacetate (**18**), and ammonium acetate in *n*-butanol, resulted in the formation of 2-amino-8-methoxy-4-(aryl)-5,6-dihydrobenzo[*h*]quinoline-3-carbonitriles **17a-c** and 8-methoxy-4-(aryl)-2-oxo-1,2,5,6-tetrahydrobenzo[*h*]quinoline-3-carbonitriles **19a-c**, respectively (Scheme 3). These compounds were also prepared in a one pot reaction by the treatment of compound **1** with aldehydes **8a-c** and malononitrile (**16**) or ethyl cyanoacetate (**18**), in the presence of ammonium acetate in *n*-butanol.

The latter synthesized compounds **17a-c** and **19a-c** were confirmed on the basis of their elemental analysis and spectral data. The IR spectra of **17a-c** revealed the bands of the amino groups at 3437–3500 and 3318–3394 cm^{-1} in addition to absorption bands at 2204–2221 cm^{-1} corresponding to the nitrile functions, respectively. While their ^{1}H NMR spectra showed a D_2O exchangeable singlet signal of NH_2 protons at δ 6.46–6.58 ppm. The IR spectra of **19a-c** revealed the appearance of three absorption bands at 3440–3472, 2218–2219, and 1630–1632 cm^{-1} due to NH, nitrile and carbonyl groups, respectively. While their ^{1}H NMR spectra represented the NH proton as a D_2O exchangeable singlet signal at δ 12.18–12.49 ppm.

Table 1
In vitro anti-proliferative activity of the prepared compounds against HepG2, MCF-7, HCT116, Caco-2 and BHK-21 cancer cell lines.

Compound	IC_{50} (μM)[a]				
	HepG2	MCF-7	HCT116	Caco-2	BHK-21
5a	29.40 ± 1.76	NA[b]	16.33 ± 1.48	NA[b]	> 200
5b	NA[b]	NA[b]	NA[b]	23.07 ± 1.4	> 200
7	31.08 ± 2.17	21.55 ± 0.93	24.87 ± 1.49	NA[b]	> 200
12a	NA[b]	18.84 ± 1.33	NA[b]	11.96 ± 0.62	> 200
12b	NA[b]	12.35 ± 0.74	NA[b]	16.19 ± 1.32	> 200
12c	NA[b]	14.82 ± 1.36	NA[b]	23.33 ± 1.20	> 200
13a	15.60 ± 0.79	11.35 ± 1.09	NA[b]	28.37 ± 1.99	> 200
13b	15.69 ± 1.29	13.86 ± 1.11	NA[b]	20.39 ± 2.04	> 200
13c	7.84 ± 0.47	19.35 ± 1.94	NA[b]	21.44 ± 1.32	> 200
15a	NA[b]	10.20 ± 0.61	13.50 ± 0.69	NA[b]	> 200
15b	16.51 ± 1.16	17.89 ± 1.26	12.38 ± 1.24	NA[b]	> 200
15c	24.76 ± 1.94	7.70 ± 0.39	23.66 ± 1.69	NA[b]	> 200
17a	15.67 ± 0.94	12.03 ± 1.22	17.35 ± 1.42	NA[b]	> 200
17b	18.58 ± 2.42	17.55 ± 1.59	20.39 ± 1.01	NA[b]	> 200
17c	13.68 ± 1.24	14.45 ± 0.89	12.91 ± 1.55	NA[b]	> 200
19a	NA[b]	18.14 ± 1.63	NA[b]	NA[b]	> 200
19b	NA[b]	7.21 ± 0.43	NA[b]	NA[b]	> 200
19c	NA[b]	13.65 ± 0.96	NA[b]	NA[b]	> 200
Dox.	1.95 ± 0.11	1.10 ± 0.06	0.63 ± 0.03	3.04 ± 0.18	
Erlotinib	10.19 ± 0.51	5.06 ± 0.27	13.22 ± 0.71	19.13 ± 0.88	

[a] IC_{50} values are the mean ± SD of three separate experiments.
[b] NA: Compounds having IC_{50} value > 50 μM.

2.2. Anticancer activity

2.2.1. In vitro anti-proliferative activity against HEPG2, MCF-7, HCT116 and Caco-2 cell lines

The anticancer activity of the synthesized compounds (**5a, 5b**, **7**, **12a-c**, **13a-c**, **15a-c**, **17a-c** and **19a-c**) was evaluated against four cancerous cell lines; liver carcinoma (HepG2), breast carcinoma (MCF-7), colon carcinoma (HCT116 and Caco-2) cell lines, using (SRB) colorimetric assay. Doxorubicin and Erlotinib were included in the experiments as reference cytotoxic compounds for all the tested cell lines. The results were expressed as median growth inhibitory concentration (IC_{50}) values, which represent the concentration of a drug that is required for 50% inhibition of cell growth after 48 h of incubation, compared to untreated controls (Table 1).

From IC_{50} values, we can deduce that the synthesized compounds showed good to moderate cytotoxic activity against the tested cancer cell lines. Regarding the activity against HepG2 cells, compound **13c** was the most active derivative with IC_{50} value equals 7.84 μM Also, compounds **13a**, **13b**, **15b**, **17a**, **17b** and **17c** showed good activity with IC_{50} = 15.60, 15.69, 16.51, 15.67, 18.58 and 13.68 μM, respectively. Whereas, compounds **5a**, **7** and **15c** exhibited a moderate activity with IC_{50} = 29.40, 31.08 and 24.76 μM, respectively. Interestingly, MCF-7 cell line emerged as the most sensitive one to the influence of the target compounds as all of the tested compounds except **5a** and **5b** showed potent to moderate activity with IC_{50} values ranging from 7.21 to 21.55 μM. In particular, compounds **15c** and **19b** were the most active compounds through this study with IC_{50} values equal 7.70 and 7.21 μM, respectively.

On the other hand, compounds **5a**, **7**, **15a**, **15b**, **15c**, **17a**, **17b**, **17c** displayed a moderate activity against HCT116 cells with IC_{50} range from 12.38 to 24.87 μM. Whereas, compounds **5b**, **12a**, **12b**, **12c**, **13a**, **13b** and **13c** had promising activity with IC_{50} = 23.07, 11.96, 16.19, 23.33, 28.37, 20.39 and 21.44 μM, respectively, towards Caco-2 cell line. It's also noteworthy that some compounds showed selective cytotoxic activity towards the examined cell lines; such as **5b** which was selective toward Caco-2, and **19a-c** which were selective against MCF-7.

2.2.2. In vitro cytotoxicity towards normal BHK-21 fibroblast cell line

The cytotoxic activity of the target compounds was also examined towards normal BHK-21 fibroblast cells to investigate the safety of the prepared compounds, using (SRB) colorimetric assay (Table 1). All the tested compounds did not display any significant cytotoxicity towards BHK-21 cells (IC_{50} value > 200 μM, for all compounds), thereby providing a good safety profile as anticancer agents.

2.2.3. In vitro EGFR kinase assay

The most potent compounds against EGFR-expressing MCF-7 cell line **13a, 13b, 15a, 15c, 17a**, **19b, 19c** were selected to investigate their potential inhibitory activity towards EGFR by use of an ADP-Glo™ Kinase Assay. The results were reported as 50% inhibition concentration values (IC_{50}) and were summarized in Table 2. The Results revealed that the examined compounds exhibited EGFR inhibitory activity with IC_{50} values ranging from 0.13 to 3.50 μM. Compounds **15c** and **19b** were the most potent EGFR inhibitors in this study that displayed comparable potency (IC_{50} = 0.13 ± 0.01 and 0.14 ± 0.01 μM, respectively) to the reference drug Erlotinib (IC_{50} = 0.11 ± 0.01 μM). In addition, compound **13b** displayed potent EGFR inhibitory activity with IC_{50} value equals 0.49 ± 0.02 μM.

2.3. Molecular docking

Docking of the most potent EGFR-TK inhibitors (**15c** and **19b**) was

Table 2
IC_{50} values of the EGFR inhibitory activity of compounds (**13a**, **13b**, **15a**, **15c**, **17a**, **19b** and **19c**).

Compound	IC_{50} (μM)[a] EGFR
13a	1.39 ± 0.08
13b	0.48 ± 0.02
15a	3.50 ± 0.18
15c	0.13 ± 0.01
17a	0.74 ± 0.07
19b	0.14 ± 0.01
19c	1.44 ± 0.12
Erlotinib	0.11 ± 0.01

[a] IC_{50} values are the mean ± SD of three separate experiments.

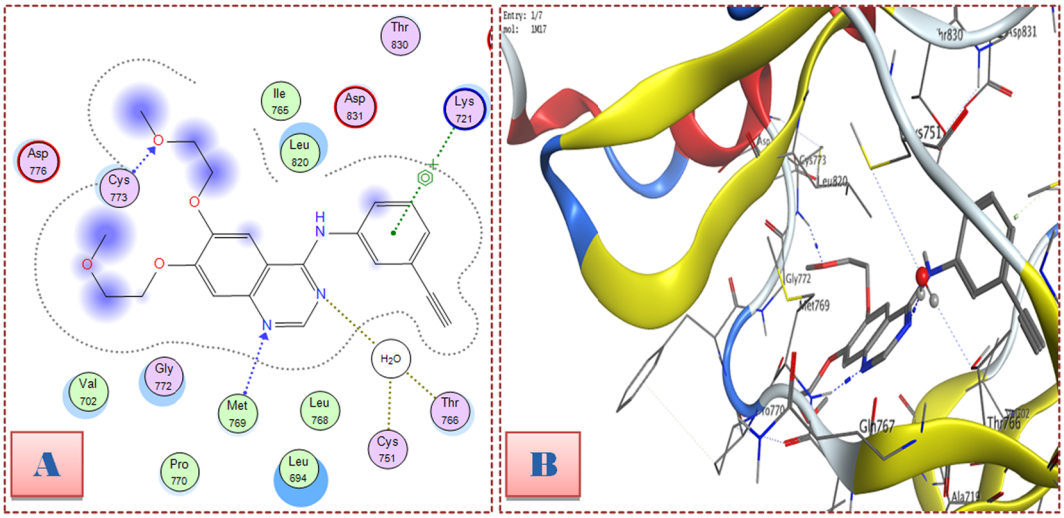

Fig. 3. 2D diagram (A) and 3D representation (B) of Erlotinib showing its binding interaction with the EGFR active site.

carried out to study their pattern of binding and potential binding interactions into the ATP binding site of the EGFR kinase domain. The ability of compounds **15c** and **19b** to interact with the key amino acids in the ATP binding site of EGFR-TK rationalized their promising antitumor activities.

Erlotinib (the co-crystallized ligand for PDB ID: 1 M17) showed three hydrogen bonding interactions between N^1 of quinazoline moiety and Met769, a water mediated hydrogen bond between N^3 of quinazoline and Thr766 [36], and between oxygen atom of the ether side chain and Cys773, in addition to a π-cation interaction between the phenyl ring of 4-anilino moiety and Lys721 (Fig. 3).

Docking simulations for compounds **15c** and **19b** showed that they fit into the EGFR active site almost at the same manner of Erlotinib with comparable docking scores (−7.97 kcal/mol for Erlotinib, −6.60 and −5.86 kcal/mol for compounds **15c** and **19b**, respectively).

Compound **15c** displayed two essential interactions, as Erlotinib, through two hydrogen bonding between N^1 and N^3 of quinazoline moiety, and Met769 and Thr766, respectively. In addition, Methoxy group showed hydrogen bonding interaction with Lys721 and a π-cation interaction with Phe699 (Fig. 4).

Furthermore, compound **19b** revealed two hydrogen bonds between the carbonyl group and Met769, and a water mediated between nitrile group and Thr766, in addition to, a π-cation interaction between pyridone ring and Gly772 (Fig. 5).

3. Conclusion

In summary, this study reports the facile synthesis of potent and selective series of benzo[*g*]indazole (**5a, b**), benzo[*h*]quinazoline (**7**, **12a-c**, **13a-c** and **15a-c**), and benzo[*h*]quinoline (**17a-c** and **19a-c**) derivatives. All the prepared compounds were examined for their anticancer activity against four cancer cell lines; HepG2, MCF-7, HCT116 and Caco-2. Compounds **15c** and **19b** showed a promising anticancer activity against MCF-7 cell line as they were the most potent derivatives with IC_{50} values = 7.70 ± 0.39 and 7.21 ± 0.43 μM, respectively. Also, compounds **15c** and **19b** displayed potent inhibitory activity towards EGFR-TK (IC_{50} = 0.13 ± 0.01 and 0.14 ± 0.01 μM, respectively). Furthermore, the molecular docking study explored the binding mode and possible interactions between the synthesized compounds and ATP binding site of EGFR kinase domain.

4. Experimental

4.1. Chemistry

4.1.1. General

Melting points were measured with a Stuart melting point apparatus and were uncorrected. Infrared spectra were recorded on Shimadzu FT-IR spectrophotometer as potassium bromide discs. Mass spectra (MS) were performed at 70 e.v by GCMS-QP1000 EX spectrometer using the

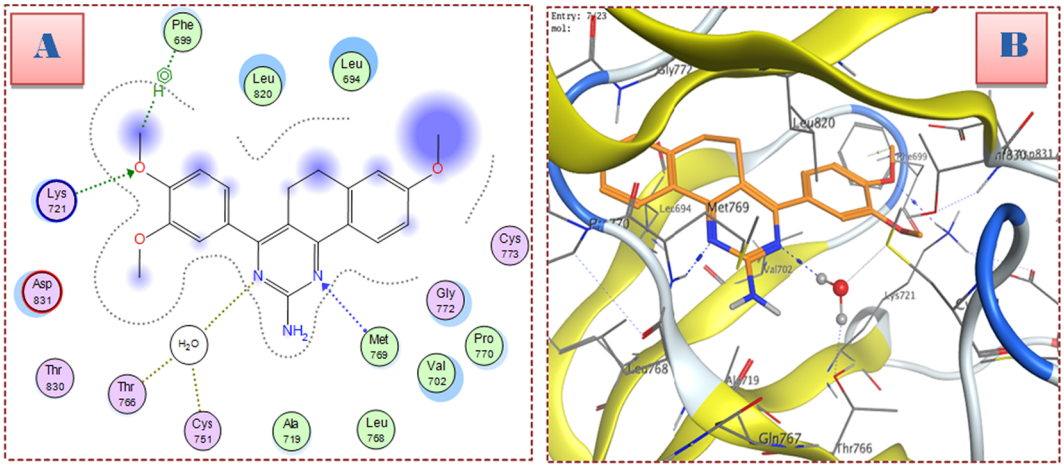

Fig. 4. 2D diagram (A) and 3D representation (B) of compound **15c** showing its binding interaction with the EGFR active site.

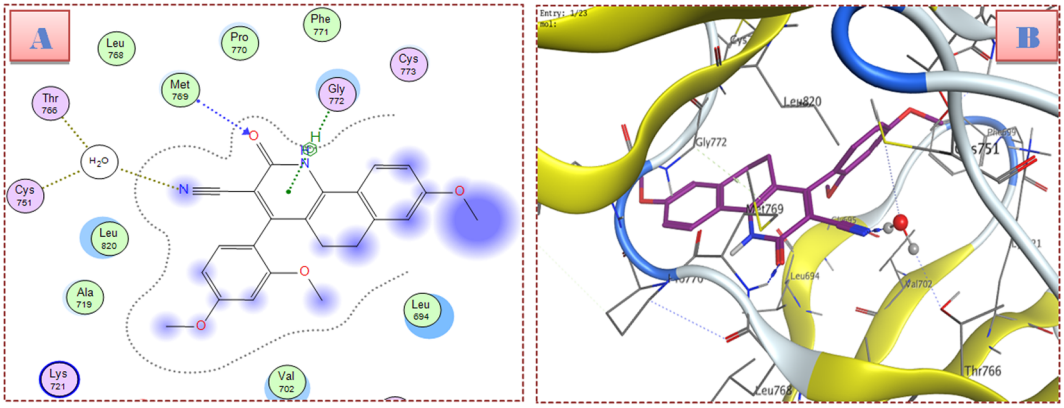

Fig. 5. 2D diagram (A) and 3D representation (B) of compound **19b** showing its binding interaction with the EGFR active site.

Electron Ionization Technique (EI). NMR Spectra were recorded on Mercury spectrometer at 300 MHz or Bruker NMR spectrometer at 400 MHz. ^{1}H spectra were run at 300 or 400 MHz, while ^{13}C spectra were run at 75 MHz in deuterated dimethyl sulfoxide (DMSO-d_6). Chemical shifts are expressed in values (pp*m*) using the solvent peak as internal standard. All coupling constant (*J*) values are given in hertz. The abbreviations used are as follows: s, singlet; d, doublet; m, multiplet. Elemental analyses were carried out at the Regional Center for Mycology and Biotechnology, Al-Azhar University, Cairo, Egypt. Analytical thin layer chromatography (TLC) on silica gel plates containing UV indicator was employed routinely to follow the course of reactions and to check the purity of products. All reagents and solvents were purified and dried by standard techniques.

4.1.2. Synthesis of 2-acetyl-6-methoxy-3,4-dihydronaphthalen-1(2H)-one (3)

6-Methoxy-3,4-dihydronaphthalen-1(2*H*)-one (**1**) (1.76 g, 10 mmol) was added to a sodium ethoxide solution prepared from sodium metal (0.46 g, 20 mmol) and absolute ethanol (20 mL). After stirring for 15 min, ethyl acetate (**2**) (1.62 g, 20 mmol) was added and the mixture was refluxed for 4 h. After cooling, the solution mixture was poured onto cold water; neutralized with acetic acid (10%) and left in the refrigerator overnight. The solid product was collected by filtration, washed with diethyl ether, dried and finally crystallized from ethanol to give compound **3** as brown crystals in 84% yield, m.p. 56–58 °C (reported m.p. 59–60 °C) [37]; IR (KBr, ν cm^{-1}): 3174 (OH); ^{1}H NMR (DMSO-d_6, 400 MHz) δ ppm: 2.18, 2.25 (s, 3H, C$\underline{H}_3$), 2.56–2.60 (m, 2H, C$\underline{H}_2$), 2.81–2.96 (m, 2H, C$\underline{H}_2$), 3.83 (s, 3H, OC$\underline{H}_3$), 6.89–6.93 (m, 2H, H-5 and H-7), 7.78, 7.83 (d, J = 8.4 Hz, 1H, H-8); 16.57 (s, 1H, OH, D_2O exchangeable); ^{13}C NMR (DMSO-d_6, 75 MHz) δ ppm: 22.0 and 22.5 (tautomeric C3), 25.0 (C$\underline{H}_3$), 27.3 and 27.7 (tautomeric C4), 55.3 (OC$\underline{H}_3$), 104.7 (*C*2), 112.6, 113.4, 123.5, 127.5, 143.7, 162.5, 178.5, 190.0 (C$\underline{=}$O); MS (EI) *m/z* (%): 218.04 (M$^+$, 19.2), 63.99 (100); Anal. Calcd. for $C_{13}H_{14}O_3$ (218.25): C, 71.54; H, 6.47; Found C, 71.62; H, 6.51.

*4.1.3. Synthesis of benzo[g]indazoles **5a,b***

*4.1.3.1. 7-Methoxy-3-methyl-4,5-dihydro-2H-benzo[g]indazole (**5a**).* To a solution of 2-acetyl-6-methoxy-3,4-dihydronaphthalen-1(2*H*)-one (**3**) (0.218 g, 1 mmol) in absolute ethanol (50 mL), hydrazine hydrate (**4a**) (99%, 0.2 g, 4 mmol) was added. The reaction mixture was refluxed for 3 h, then left to cool and pour onto ice. The formed precipitate was filtered and crystallized from ethanol to afford the corresponding indazole **5a** as white powder in 79% yield, m.p. 165–167 °C; IR (KBr, ν cm^{-1}): 3186 (NH), 1617 (C$\underline{=}$N); ^{1}H NMR (DMSO-d_6, 400 MHz) δ ppm: 2.16 (s, 3H, C$\underline{H}_3$), 2.55–2.59 (m, 2H, C$\underline{H}_2$), 2.82–2.85 (m, 2H, C$\underline{H}_2$), 3.76 (s, 3H, OC$\underline{H}_3$), 6.81 (d, J = 7.6 Hz, 1H, H-8), 6.86 (s, 1H, H-6), 7.55 (s, 1H, H-9), 12.19 and 12.64 (2 s, 1H, tautomeric NH, D_2O exchangeable); MS (EI) *m/z* (%): 214.15 (M$^+$, 2.1), 77.08 (100); Anal. Calcd. for $C_{13}H_{14}N_2O$ (214.26): C, 72.87; H, 6.59; N, 13.07; Found C, 72.79; H, 6.54; N, 13.02.

*4.1.3.2. 7-Methoxy-3-methyl-2-phenyl-4,5-dihydro-2H-benzo[g]indazole (**5b**).* To a solution compound **3** (0.218 g, 1 mmol) in glacial acetic acid (50 mL), phenyl hydrazine (**4b**) (0.11 g, 1 mmol) was added. The reaction mixture was refluxed for 5 h, then left to cool and pour onto ice. The formed precipitate was filtered and crystallized from ethanol to give indazole **5b** as buff powder in 60% yield, m.p. 114–116 °C; IR (KBr, ν cm^{-1}): 1598 (C$\underline{=}$N); ^{1}H NMR (DMSO-d_6, 400 MHz) δ ppm: 2.19 (s, 3H, C$\underline{H}_3$), 2.57–2.60 (m, 2H, C$\underline{H}_2$), 2.90–2.93 (m, 2H, C$\underline{H}_2$), 3.72 (s, 3H, OC$\underline{H}_3$), 6.61 (s, 2H, Ar H), 6.95 (s, 1H, Ar H), 7.41–7.53 (m, 5H, Ar H); ^{13}C NMR (DMSO-d_6, 75 MHz) δ ppm: 11.2 (C$\underline{H}_3$), 18.5 (C4), 30.1 (C5), 54.9 (OC$\underline{H}_3$), 111.2, 111.2, 114.5 (2C), 116.6, 119.4, 123.3, 125.2, 127.7, 129.1, 137.2, 138.8, 140.5, 144.9, 158.3; MS (EI) *m/z* (%): 290.21 (M$^+$, 6.73), 57.11 (100); Anal. Calcd. for $C_{19}H_{18}N_2O$ (290.36): C, 78.59; H, 6.25; N, 9.65; Found C, 78.48; H, 6.21; N, 9.59.

*4.1.4. 8-Methoxy-4-methyl-5,6-dihydrobenzo[h]quinazolin-2-amine (**7**)*

To a solution mixture of 2-acetyl-6-methoxy-3,4-dihydronaphthalen-1(2*H*)-one (**3**) (0.218 g, 1 mmol) and guanidine hydrochloride (**6**) (0.19 g, 2 mmol) in absolute ethanol (30 mL), potassium hydroxide (0.17 g, 3 mmol) was added and the mixture was heated under reflux for 24 h. The produced product was filtered, washed with ethanol, dried and crystallized from EtOH/DMF to give compound **7** as grey powder in 82% yield, m.p. > 300 °C; IR (KBr, ν cm^{-1}): 3471 and 3298 (NH$_2$), 1632 (C$\underline{=}$N); ^{1}H NMR (DMSO-d_6, 400 MHz) δ ppm: 2.26 (s, 3H, CH$_3$), 2.68–2.71 (m, 2H, C$\underline{H}_2$), 2.81–2.85 (m, 2H, C$\underline{H}_2$), 3.81 (s, 3H, OC$\underline{H}_3$), 6.20 (s, 2H, NH$_2$, D_2O exchangeable), 6.86–6.91 (m, 2H, H-7 and H-9), 8.04 (d, J = 8.4 Hz, 1H, H-10); MS (EI) *m/z* (%): 241.26 (M$^+$, 3.15), 57.09 (100); Anal. Calcd. for $C_{14}H_{15}N_3O$ (241.29): C, 69.69; H, 6.27; N, 17.41; Found C, 69.74; H, 6.32; N, 17.52.

*4.1.5. General procedure for the synthesis of 6-methoxy-2-(arylidene)-3,4-dihydronaphthalen-1(2H)-ones **9a-c***

A mixture of 6-methoxy-3,4-dihydronaphthalen-1(2*H*)-one (**1**) (1.76 g, 10 mmol), the appropriate aldehyde **8a-c** (10 mmol) and 10% sodium hydroxide solution (10%, 15 mL) in ethanol (30 mL) was stirred for 12 h at room temperature. The separated precipitate was filtered, washed with water and crystallized from ethanol to yield compounds **9a-c**, respectively.

*4.1.5.1. 6-Methoxy-2-(4-methoxybenzylidene)-3,4-dihydronaphthalen-1(2H)-one (**9a**).* White powder in 85% yield, m.p. 141–142 °C (reported m.p. 139.5 °C) [38]; IR (KBr, ν cm^{-1}): 1663 (C$\underline{=}$O); ^{1}H NMR (DMSO-d_6, 300 MHz) δ ppm: 2.88–2.92 (m, 2H, C$\underline{H}_2$), 3.04–3.08 (m, 2H, C$\underline{H}_2$), 3.80 (s, 3H, OC$\underline{H}_3$), 3.84 (s, 3H, OC$\underline{H}_3$), 6.88 (d,

J = 2.4 Hz, 1H, H-5), 6.93 (dd, *J* = 8.7, 2.4 Hz, 1H, H-7), 7.02 (d, *J* = 8.7 Hz, 2H, H-3′ and H-5′), 7.48 (d, *J* = 8.7 Hz, 2H, H-2′ and H-6′), 7.63 (s, 1H, −C=H), 7.92 (d, *J* = 8.7 Hz, 1H, H-8); ^{13}C NMR (DMSO-d_6, 75 MHz) *δ* ppm: 26.6 (C3), 28.1 (C4), 55.1 (OCH$_3$), 55.4 (OCH$_3$), 112.2, 113.4, 114.0 (2C), 126.4, 127.7, 129.7, 131.5 (2C), 133.4, 134.8, 145.6, 159.5, 163.0, 185.2 (C=O); MS (EI) *m/z* (%): 294.16 (M$^+$, 7.41), 107.12 (1 0 0); Anal. Calcd. for $C_{19}H_{18}O_3$ (294.34): C, 77.53; H, 6.16; Found C, 77.62; H, 6.19.

*4.1.5.2. 2-(2,4-Dimethoxybenzylidene)-6-methoxy-3,4-dihydronaphthalen-1(2H)-one (**9b**).* Yellow powder in 77% yield, m.p. 112–114 °C (reported m.p. 114 °C) [39]; IR (KBr, *ν* cm^{-1}): 1654 (C=O); ^{1}H NMR (DMSO-d_6, 300 MHz) *δ* ppm: 2.87–2.89 (m, 2H, CH$_2$), 2.94–2.96 (m, 2H, CH$_2$), 3.81 (s, 3H, OCH$_3$), 3.83 (s, 3H, OCH$_3$), 3.84 (s, 3H, OCH$_3$), 6.58 (dd, *J* = 8.4, 2.4 Hz, 1H, H-5′), 6.63 (d, *J* = 2.4 Hz, 1H, H-3′), 6.87 (d, *J* = 2.4 Hz, 1H, H-5), 6.93 (dd, *J* = 8.7, 2.4 Hz, 1H, H-7), 7.30 (d, *J* = 8.4 Hz, 1H, H-6′), 7.75 (s, 1H, −C=H), 7.90 (d, *J* = 8.7 Hz, 1H, H-8); ^{13}C NMR (DMSO-d_6, 75 MHz) *δ* ppm: 26.9 (C3), 28.4 (C4), 55.2 (OCH$_3$), 55.3 (OCH$_3$), 55.5 (OCH$_3$), 98.2, 104.9, 112.2, 113.4, 116.6, 123.9, 126.5, 129.7, 130.6, 133.3, 145.7, 159.2, 161.4, 162.7, 185.3 (C=O); MS (EI) *m/z* (%): 324.45 (M$^+$, 3.38), 177.15 (100); Anal. Calcd. for $C_{20}H_{20}O_4$ (324.37): C, 74.06; H, 6.22; Found C, 74.16; H, 6.28.

*4.1.5.3. 2-(3,4-Dimethoxybenzylidene)-6-methoxy-3,4-dihydronaphthalen-1(2H)-one (**9c**).* Yellow crystals in 75% yield, m.p. 112 °C (reported m.p. 112 °C) [40]; IR (KBr, *ν* cm^{-1}): 1660 (C=O); ^{1}H NMR (DMSO-d_6, 400 MHz) *δ* ppm: 2.89–2.93 (m, 2H, CH$_2$), 3.08–3.12 (m, 2H, CH$_2$), 3.80 (s, 3H, OCH$_3$), 3.81 (s, 3H, OCH$_3$), 3.85 (s, 3H, OCH$_3$), 6.90 (s, 1H, H-5), 6.94 (d, *J* = 10 Hz, 1H, H-7), 7.03 (d, *J* = 8.8 Hz, 1H, H-5′), 7.11 (m, 2H, H-2′ and H-6′), 7.65 (s, 1H, −C=H), 7.92 (d, *J* = 7.2 Hz, 1H, H-8); ^{13}C NMR (DMSO-d_6, 75 MHz) *δ* ppm: 26.6 (C3), 28.2 (C4), 55.3 (OCH$_3$), 55.4 (OCH$_3$), 55.6 (OCH$_3$), 111.6, 112.2, 113.4, 113.8, 123.0, 126.4, 128.0, 129.6, 133.6, 135.1, 145.6, 148.5, 149.4, 163.0, 185.2 (C=O); MS (EI) *m/z* (%): 324.57 (M$^+$, 7.72), 88.05 (100); Anal. Calcd. for: $C_{20}H_{20}O_4$ (324.37): C, 74.06; H, 6.22; Found C, 74.21; H, 6.27.

*4.1.6. General procedure for the synthesis of benzo[h]quinazolines **12a-c** and **13a-c***

To a mixture of 6-methoxy-2-(arylidene)-3,4-dihydronaphthalen-1(2*H*)-ones **9a-c** (1 mmol) and urea/thiourea **10a, b** (1 mmol), in ethanol (50 mL), potassium hydroxide (0.11 g, 2 mmol) was added. The mixture was heated under reflux for 24 h. The formed product was filtered, dissolved in cold water and acidified with dilute hydrochloric acid. The formed product was filtered, washed with water, dried and crystallized from EtOH/DMF to give the corresponding benzo[*h*]quinazolines **12a-c** and **13a-c**, respectively.

*4.1.6.1. 8-Methoxy-4-(4-methoxyphenyl)-5,6-dihydrobenzo[h]quinazolin-2(3H)-one (**12a**).* Buff powder in 65% yield, m.p. 199–201 °C (reported m.p. 199–201 °C) [41]; IR (KBr, *ν* cm^{-1}): 3426 (NH), 1630 (C=O); ^{1}H NMR (DMSO-d_6, 300 MHz) *δ* ppm: 2.65–2.68 (m, 2H, CH$_2$), 2.72–2.73 (m, 2H, CH$_2$), 3.81 (s, 3H, OCH$_3$), 3.84 (s, 3H, OCH$_3$), 6.84 (d, *J* = 2.1 Hz, 1H, H-7), 6.90 (d, *J* = 8.4 Hz, 1H, H-9), 7.02 (d, *J* = 8.4 Hz, 2H, H-3′ and H-5′), 7.49 (d, *J* = 8.4 Hz, 2H, H-2′ and H-6′), 8.11 (d, *J* = 8.4 Hz, 1H, H-10); MS (EI) *m/z* (%): 334.07 (M$^+$, 4.47), 71.08 (100); Anal. Calcd. for $C_{20}H_{18}N_2O_3$ (334.37): C, 71.84; H, 5.43; N, 8.38; Found C, 71.93; H, 5.47; N, 8.44.

*4.1.6.2. 4-(2,4-Dimethoxyphenyl)-8-methoxy-5,6-dihydrobenzo[h]quinazolin-2(3H)-one (**12b**).* Pale yellow powder in 60% yield, m.p. 253–255 °C; IR (KBr, *ν* cm^{-1}): 3421 (NH), 1632 (C=O); ^{1}H NMR (DMSO-d_6, 300 MHz) *δ ppm*: 2.38–2.42 (m, 2H, CH$_2$), 2.73–2.78 (m, 2H, CH$_2$), 3.79 (s, 3H, OCH$_3$), 3.83 (s, 3H, OCH$_3$), 3.84 (s, 3H, OCH$_3$), 6.64 (dd, *J* = 8.1, 1.8 Hz, 1H, H-5′), 6.70 (d, *J* = 1.8 Hz, 1H, H-3′), 6.87 (d, *J* = 2.1 Hz, 1H, H-7), 6.95 (dd, *J* = 8.7, 2.4 Hz, 1H, H-9), 7.26 (d, *J* = 8.4 Hz, 1H, H-6′), 8.12 (d, *J* = 8.7 Hz, 1H, H-10), 11.50 (s, 1H, NH, D_2O exchangeable); MS (EI) *m/z* (%): 364.13 (M$^+$, 4.85), 130.12 (100); Anal. Calcd. for $C_{21}H_{20}N_2O_4$ (364.39): C, 69.22; H, 5.53; N, 7.69; Found C, 69,13; H, 5.50; N, 7.64.

*4.1.6.3. 4-(3,4-Dimethoxyphenyl)-8-methoxy-5,6-dihydrobenzo[h]quinazolin-2(3H)-one (**12c**).* Pale yellow powder in 50% yield, m.p. 146–148 °C (reported m.p. 148–150 °C) [41]; IR (KBr, *ν* cm^{-1}): 3423 (NH), 1631 (C=O); ^{1}H NMR (DMSO-d_6, 400 MHz) *δ* ppm: 2.70 and 2.77 (2 m, 4H, 2CH$_2$), 3.69 and 3.83 (2 s, 9H, 3OCH$_3$), 6.89 (s, 1H, H-7), 6.95 (d, *J* = 9.6 Hz, 1H, H-9), 7.07–7.16 (m, 3H, H2′, H-5′ and H-6′), 8.12 (d, *J* = 10.4 Hz, 1H, H-10); ^{13}C NMR (DMSO-d_6, 75 MHz) *δ* ppm: 23.0 (C5), 27.9 (C6), 55.1 (OCH$_3$), 55.4 (OCH$_3$), 55.7 (OCH$_3$), 109.3, 111.4 (2C), 112.6 (2C), 112.8, 113.0, 120.8, 121.9 (2C), 124.9, 128.0, 142.6, 148.5, 150.3, 162.1; MS (EI) *m/z* (%): 364.2 (M$^+$, 10.79), 83.11 (100); Anal. Calcd. for $C_{21}H_{20}N_2O_4$ (364.39): C, 69.22; H, 5.53; N, 7.69; Found C, 69.34; H, 5.58; N, 7.75.

*4.1.6.4. 8-Methoxy-4-(4-methoxyphenyl)-3,4,5,6-tetrahydrobenzo[h]quinazoline-2(1H)-thione (**13a**).* White powder in 40% yield, m.p. 234–236 °C (reported m.p. 234–237 °C) [41]; IR (KBr, *ν* cm^{-1}): 3197 and 3113 (2NH), 1250 (C=S); ^{1}H NMR (DMSO-d_6, 400 MHz) *δ* ppm: 1.82–1.84 and 2.07–2.16 (2 m, 2H, CH$_2$), 2.55–2.60 and 2.65–2.74 (2 m, 2H, CH$_2$), 3.73 (s, 3H, OCH$_3$), 3.74 (s, 3H, OCH$_3$), 4.86 (s, 1H, pyrimidine-C4), 6.76–6.78 (m, 2H, H-7 and H-9), 6.92 (d, *J* = 6.4 Hz, 2H, H-3′ and H-5′), 7.22 (d, *J* = 8.8 Hz, 2H, H-2′ and H-6′), 7.60 (d, *J* = 8.4 Hz, 1H, H-10), 8.95 (s, 1H, NH, D_2O exchangeable), 9.60 (s, 1H, NH, D_2O exchangeable); ^{13}C NMR (DMSO-d_6, 75 MHz) *δ ppm*: 23.5 (C5), 27.7 (C6), 55.0 (2OCH$_3$), 57.8 (C4), 108.6, 110.7, 113.8, 113.9 (2C), 120.5, 122.8, 126.2, 128.1 (2C), 135.0, 137.3, 158.8, 158.9, 173.9 (C=S); MS (EI) *m/z* (%): 352.33 (M$^+$, 13.53), 45.08 (1 0 0); Anal. Calcd. for $C_{20}H_{20}N_2O_2S$ (352.45): C, 68.16; H, 5.72; N, 7.95; Found C, 68.03; H, 5.68; N, 7.88.

*4.1.6.5. 4-(2,4-Dimethoxyphenyl)-8-methoxy-3,4,5,6-tetrahydrobenzo[h]quinazoline-2(1H)-thione (**13b**).* White powder in 45% yield, m.p. 160–162 °C; IR (KBr, *ν* cm^{-1}): 3194 (2NH), 1252 (C=S); ^{1}H NMR (DMSO-d_6, 400 MHz) *δ* ppm: 1.79–1.87 and 2.07–2.15 (2 m, 2H, CH$_2$), 2.55–2.59 and 2.65–2.73 (2 m, 2H, CH$_2$), 3.74 (s, 6H, 2OCH$_3$), 3.79 (s, 3H, OCH$_3$), 5.20 (s, 1H, pyrimidine-C4), 6.55–6.56 (m, 2H, H-3′ and H-5′), 6.75 (s, 2H, H-7 and H-9), 7.08 (d, *J* = 8.8 Hz, 1H, H6′), 7.57 (d, *J* = 12 Hz, 1H, *H*10), 8.60 (s, 1H, NH, D_2O exchangeable), 9.54 (s, 1H, NH, D_2O exchangeable); ^{13}C NMR (DMSO-d_6, 75 MHz) *δ* ppm: 23.3 (C5), 27.8 (C6), 54.9 (C4), 55.2 (OCH$_3$), 55.5 (OCH$_3$), 55.7 (OCH$_3$), 98.5, 105.5, 108.6, 110.8, 113.8, 120.8, 122.7, 123.4, 126.4, 128.6, 137.4, 157.4, 158.8, 160.2, 174.6 (C=S); MS (EI) *m/z* (%): 382.03 (M$^+$, 27.35), 55.20 (1 0 0); Anal. Calcd. for $C_{21}H_{22}N_2O_3S$ (382.48): C, 65.95; H, 5.80; N, 7.32; Found C, 65.87; H, 5.76; N, 7.26.

*4.1.6.6. 4-(3,4-Dimethoxyphenyl)-8-methoxy-3,4,5,6-tetrahydrobenzo[h]quinazoline-2(1H)-thione (**13c**).* White powder in 59% yield, m.p. 253–255 °C (reported m.p. 253–255 °C) [41]; IR (KBr, *ν* cm^{-1}): 3186 (2NH), 1257 (C=S); ^{1}H NMR (DMSO-d_6, 400 MHz) *δ* ppm: 1.87–1.91 and 2.11–2.20 (2 m, 2H, CH$_2$), 2.57–2.63 and 2.67–2.75 (2 m, 2H, CH$_2$), 3.74 (s, 6H, 2OCH$_3$), 3.76 (s, 3H, OCH$_3$), 4.87 (s, 1H, pyrimidine-C4), 6.78 (s, 2H, H-7 and H-9), 6.83 (d, *J* = 6.8 Hz, 1H, H-5′), 6.92–6.97 (m, 2H, H-2′ and H-6′), 7.62 (d, *J* = 7.6 Hz, 1H, H-10), 8.95 (s, 1H, NH, D_2O exchangeable), 9.64 (s, 1H, NH, D_2O exchangeable); ^{13}C NMR (DMSO-d_6, 75 MHz) *δ* ppm: 23.5 (C-5), 27.7 (C-6), 55.0 (OCH$_3$), 55.5 (OCH$_3$), 55.5 (OCH$_3$), 58.1 (C-4), 108.5, 110.7, 111.1, 112.0, 113.8, 119.0, 120.6, 122.8, 126.4, 135.4, 137.4, 148.5, 148.7, 158.8, 174.0 (C=S); MS (EI) *m/z* (%): 382.17 (M$^+$, 26.18), 40.18 (100); Anal. Calcd. for $C_{21}H_{22}N_2O_3S$ (382.48): C, 65.95; H, 5.80; N, 7.32; Found C, 65.99; H, 5.84; N, 7.36.

*4.1.7. General procedure for the synthesis of benzo[h]quinazolines **15a-c***

These compounds were prepared by the same method for synthesis of compound **7** by using the appropriate 6-methoxy-2-(arylidene)-3,4-dihydronaphthalen-1(2*H*)-ones **9a-c** instead of 2-acetyl-6-methoxy-3,4-dihydronaphthalen-1(2*H*)-one (**3**).

*4.1.7.1. 8-Methoxy-4-(4-methoxyphenyl)-5, 6-dihydrobenzo[h]quinazolin-2-amine (**15a**)*. Green powder in 57% yield, m.p. 152–154 °C; IR (KBr, ν cm^{-1}): 3477, 3297 (NH_2), 1609 (C═N); ^{1}H NMR (DMSO-d_6, 400 MHz) δ ppm: 2.76 (s, 4H, 2C$\underline{H}_2$), 3.82 (s, 6H, 2OC$\underline{H}_3$), 6.37 (s, 2H, NH_2, D_2O exchangeable), 6.86 (s, 1H, H-7), 6.93 (d, J = 6.4 Hz, 1H, H-9), 7.02 (d, J = 7.6 Hz, 2H, H-3′ and H-5′), 7.53 (d, J = 6.8 Hz, 2H, H-2′ and H-6′), 8.11 (d, J = 7.6 Hz, 1H, H-10); ^{13}C NMR (DMSO-d_6, 75 MHz) δ ppm: 23.8 (C-5), 28.0 (C-6), 55.1 (O$\underline{C}H_3$), 55.3 (O$\underline{C}H_3$), 112.4, 112.7, 113.0, 113.5, 126.0, 126.7, 126.8, 129.9, 130.4, 130.8, 141.3, 159.6 (C-8), 159.7, 161.0, 162.0 (C-4), 163.9 (C═N); MS (EI) *m/z* (%): 333.16 (M^+, 14.04), 191.93 (100); Anal. Calcd. for $C_{20}H_{19}N_3O_2$ (333.38): C, 72.05; H, 5.74; N, 12.60; Found C, 72.13; H, 5.79; N, 12.69.

*4.1.7.2. 4-(2,4-Dimethoxyphenyl)-8-methoxy-5,6-dihydrobenzo[h]quinazolin-2-amine (**15b**)*. Green powder in 70% yield, m.p. 206 °C; IR (KBr, ν cm^{-1}): 3436, 3305 (NH_2), 1608 (C═N); ^{1}H NMR (DMSO-d_6, 400 MHz) δ ppm: 2.33, 2.51 (2 s, 2H, C$\underline{H}_2$), 2.71 (s, 2H, C$\underline{H}_2$), 3.74 (s, 3H, OC$\underline{H}_3$), 3.81 (s, 3H, OC$\underline{H}_3$), 3.82 (s, 3H, OC$\underline{H}_3$), 6.32 (s, 2H, NH_2, D_2O exchangeable), 6.61–6.65 (m, 2H, H-3′ and H-5′), 6.84 (s, 1H, H-7), 6.92 (d, J = 8.8 Hz, 1H, H-9), 7.21 (d, J = 7.6 Hz, 1H, H-6′), 8.10 (d, J = 9.2 Hz, 1H, H-10); ^{13}C NMR (DMSO-d_6, 75 MHz) δ ppm: 23.0 (C5), 27.8 (C6), 55.1 (O$\underline{C}H_3$), 55.2 (2O$\underline{C}H_3$), 98.0 (C3′), 105.0 (C5′), 112.4, 112.7, 115.1, 120.4, 125.8, 126.6, 130.6, 141.4, 157.3, 158.4, 160.8, 160.9, 162.0 (C4), 163.1 (C═N); MS (EI) *m/z* (%): 363.05 (M^+, 5.21), 83.11 (100); Anal. Calcd. for $C_{21}H_{21}N_3O_3$ (363.41): C, 69.41; H, 5.82; N, 11.56; Found C, 69.53; H, 5.87; N, 11.63.

*4.1.7.3. 4-(3,4-Dimethoxyphenyl)-8-methoxy-5,6-dihydrobenzo[h]quinazolin-2-amine (**15c**)*. Green powder in 68% yield, m.p. 207 °C; IR (KBr, ν cm^{-1}): 3416, 3309 (NH_2), 1605 (C═N); ^{1}H NMR (DMSO-d_6, 400 MHz) δ ppm: 2.75–2.79 (m, 4H, 2C$\underline{H}_2$), 3.79 (s, 3H, OC$\underline{H}_3$), 3.81 (s, 6H, 2OC$\underline{H}_3$), 6.36 (s, 2H, NH_2, D_2O exchangeable), 6.86 (s, 1H, H-7), 6.92 (d, J = 8.8 Hz, 1H, H-9), 7.03 (d, J = 9.2 Hz, 1H, H-5′), 7.11 (d, J = 8.4 Hz, 1H, H-6′), 7.16 (s, 1H, H-2′), 8.10 (d, J = 8.8 Hz, 1H, H-10); ^{13}C NMR (DMSO-d_6, 75 MHz) δ ppm: 23.8 (C5), 28.0 (C6), 55.3 (O$\underline{C}H_3$), 55.5 (O$\underline{C}H_3$), 55.6 (O$\underline{C}H_3$), 111.0, 112.5 (2C), 112.7, 113.1, 121.5, 125.9, 126.8, 130.9, 141.3, 148.2, 149.3, 159.7, 160.9, 161.9 (C4), 164.1 (C═N); MS (EI) *m/z* (%): 363.28 (M^+, 4.31), 292.13 (100); Anal. Calcd. for $C_{21}H_{21}N_3O_3$ (363.41): C, 69.41; H, 5.82; N, 11.56; Found C, 69.34; H, 5.77; N, 11.48.

*4.1.8. General procedure for the synthesis of benzo[h]quinolines **17a-c** and **19a-c***

A mixture of the appropriate 6-methoxy-2-(arylidene)-3,4-dihydronaphthalen-1(2*H*)-ones **9a-c** (1 mmol), malononitrile (**16**) or ethyl cyanoacetate (**18**) (1 mmol), and ammonium acetate (0.77 g, 10 mmol) in *n*-butanol (40 mL) was heated under reflux for 12 h. The formed precipitate was filtered, washed with ethanol and crystallized from EtOH/DMF to yield the corresponding benzo[*h*]quinolines **17a-c** and **19a-c**, respectively. One pot reaction of compound **1** with the aldehydes **8a-c** and malononitrile (**16**) or ethyl cyanoacetate (**18**), in the presence of ammonium acetate in *n*-butanol gave **17a-c** and **19a-c**, respectively, with almost the same yields of the step-wise reaction.

*4.1.8.1. 2-Amino-8-methoxy-4-(4-methoxyphenyl)-5,6-dihydrobenzo[h]quinoline-3-carbonitrile (**17a**)*. Orange crystals in 54% yield, m.p. 199–201 °C; IR (KBr, ν cm^{-1}): 3437, 3354 (NH_2), 2204 (C≡N), 1636 (C═N); ^{1}H NMR (DMSO-d_6, 300 MHz) δ ppm: 2.50–2.52 (m, 2H, C$\underline{H}_2$), 2.70–2.73 (m, 2H, C$\underline{H}_2$), 3.82 (s, 3H, OC$\underline{H}_3$), 3.84 (s, 3H, OC$\underline{H}_3$), 6.53 (s, 2H, NH_2, D_2O exchangeable), 6.82 (d, J = 2.4 Hz, 1H, H-7), 6.92 (dd, J = 8.7, 2.7 Hz, 1H, H-9), 7.07 (dd, J = 6.9, 2.1 Hz, 2H, H-3′ and H-5′), 7.30 (dd, J = 6.9, 2.1 Hz, 2H, H-2′ and H-6′), 8.12 (d, J = 8.7 Hz, 1H, H-10); ^{13}C NMR (DMSO-d_6, 75 MHz) δ ppm: 23.9 (C5), 27.6 (C6), 55.1 (O$\underline{C}H_3$), 55.1 (O$\underline{C}H_3$), 88.0 (C3), 112.5, 112.6, 113.8 (2C), 117.1, 117.4, 126.2, 127.4, 128.1, 129.8 (2C), 141.0, 152.3, 154.0, 158.7, 159.4, 160.8 (C═N); MS (EI) *m/z* (%): 357.23 (M^+, 9.71), 152.21 (100); Anal. Calcd. for $C_{22}H_{19}N_3O_2$ (357.41): C, 73.93; H, 5.36; N, 11.76; Found C, 73.85; H, 5.31; N, 11.83.

*4.1.8.2. 2-Amino-4-(2,4-dimethoxyphenyl)-8-methoxy-5,6-dihydrobenzo[h]quinoline-3-carbonitrile (**17b**)*. Orange powder in 55% yield, m.p. 188 °C; IR (KBr, ν cm^{-1}): 3500, 3394 (NH_2), 2205 (C≡N), 1607 (C═N); ^{1}H NMR (DMSO-d_6, 300 MHz) δ ppm: 2.39–2.41 (m, 2H, C$\underline{H}_2$), 2.69–2.71 (m, 2H, C$\underline{H}_2$), 3.81 (s, 3H, OC$\underline{H}_3$), 3.82 (s, 3H, OC$\underline{H}_3$), 3.85 (s, 3H, OC$\underline{H}_3$), 6.46 (s, 2H, NH_2, D_2O exchangeable), 6.66 (dd, J = 8.1, 2.4 Hz, 1H, H-5′), 6.72 (d, J = 2.4 Hz, 1H, H-3′), 6.82 (d, J = 2.7 Hz, 1H, H-7), 6.91 (d, J = 8.7 Hz, 1H, H-9), 7.11 (d, J = 8.1 Hz, 1H, H-6′), 8.11 (d, J = 8.7 Hz, 1H, H-10); ^{13}C NMR (DMSO-d_6, 75 MHz) δ ppm: 23.8 (C5), 27.6 (C6), 55.1 (O$\underline{C}H_3$), 55.2 (O$\underline{C}H_3$), 55.5 (O$\underline{C}H_3$), 89.1 (C3), 98.7, 105.2, 112.6 (2C), 117.0, 118.5, 126.3, 127.3, 130.4 (2C), 141.1, 149.9, 153.5, 157.1, 158.6, 160.7, 161.2 (C═N); MS (EI) *m/z* (%): 387.21 (M^+, 7.34), 84.12 (100); Anal. Calcd. for $C_{23}H_{21}N_3O_3$ (387.43): C, 71.30; H, 5.46; N, 10.85; Found C, 71.45; H, 5.50; N, 10.93.

*4.1.8.3. 2-Amino-4-(3,4-dimethoxyphenyl)-8-methoxy-5,6-dihydrobenzo[h]quinoline-3-carbonitrile (**17c**)*. Orange powder in 70% yield, m.p. 169–170 °C (reported m.p. 170–172 °C) [42]; IR (KBr, ν cm^{-1}): 3476 and 3318 (NH_2), 2221 (C≡N), 1631 (C═N); ^{1}H NMR (DMSO-d_6, 400 MHz) δ ppm: 2.51 (m, 2H, C$\underline{H}_2$), 2.69–2.74 (m, 2H, C$\underline{H}_2$), 3.77 (s, 3H, OC$\underline{H}_3$), 3.80 (s, 3H, OC$\underline{H}_3$), 3.82 (s, 3H, OC$\underline{H}_3$), 6.58 (s, 2H, NH_2, D_2O exchangeable), 6.83 (s, 1H, H-7), 6.89–6.96 (m, 3H, H-9, H-2′ and H-5′), 7.08 (d, J = 7.2 Hz, 1H, H-6′), 8.11 (d, J = 10.4 Hz, 1H, H-10); ^{13}C NMR (DMSO-d_6, 75 MHz) δ ppm: 23.9 (C5), 27.7 (C6), 55.1 (O$\underline{C}H_3$), 55.4 (O$\underline{C}H_3$), 55.6 (O$\underline{C}H_3$), 88.0 (C3), 111.6, 112.4, 112.6, 117.1, 117.4, 120.2, 120.9, 126.3, 127.4, 128.3, 141.0, 148.4, 149.0, 152.5, 154.0, 158.7, 160.8 (C═N); MS (EI) *m/z* (%): 387.26 (M^+, 62.61), 108.21 (100); Anal. Calcd. for $C_{23}H_{21}N_3O_3$ (387.43): C, 71.30; H, 5.46; N, 10.85; Found C, 71.47; H, 5.51; N, 10.92.

*4.1.8.4. 8-Methoxy-4-(4-methoxyphenyl)-2-oxo-1,2,5,6-tetrahydrobenzo[h]quinoline-3-carbonitrile (**19a**)*. Yellow powder in 62% yield, m.p. > 300 °C; IR (KBr, ν cm^{-1}): 3472 (NH), 2218 (C≡N), 1630 (C═O); ^{1}H NMR (DMSO-d_6, 300 MHz) δ ppm: 2.35–2.39 (m, 2H, C$\underline{H}_2$), 2.69–2.74 (m, 2H, C$\underline{H}_2$), 3.82 (s, 3H, OC$\underline{H}_3$), 3.83 (s, 3H, OC$\underline{H}_3$), 6.90 (d, J = 2.4 Hz, 1H, H-7), 6.94 (dd, J = 8.4, 2.4 Hz, 1H, H-9), 7.08 (d, J = 8.7 Hz, 2H, H-3′ and H-5′), 7.34 (d, J = 8.7 Hz, 2H, H-2′ and H-6′), 8.02 (d, J = 8.7 Hz, 1H, H-10), 12.45 (s, 1H, NH, D_2O exchangeable); ^{13}C NMR (DMSO-d_6, 75 MHz) δ ppm: 23.4 (C5), 27.7 (C6), 55.1 (O$\underline{C}H_3$), 55.4 (O$\underline{C}H_3$), 112.5, 112.7, 113.1, 113.4, 113.8, 114.2, 116.6, 120.6, 127.0, 127.2, 127.5, 129.2, 129.8, 141.6, 159.3, 159.8, 161.0, 161.6; MS (EI) *m/z* (%): 358.27 (M^+, 15.36), 236.28 (100); Anal. Calcd. for $C_{22}H_{18}N_2O_3$ (358.40): C, 73.73; H, 5.06; N, 7.82; Found C, 73.67; H, 5.01; N, 7.76.

*4.1.8.5. 4-(2,4-Dimethoxyphenyl)-8-methoxy-2-oxo-1,2,5,6-tetrahydrobenzo[h]quinoline-3-carbonitrile (**19b**)*. Yellow powder in 68% yield, m.p. > 300 °C; IR (KBr, ν cm^{-1}): 3440 (NH), 2219 (C≡N), 1630 (C═O); ^{1}H NMR (DMSO-d_6, 300 MHz) δ ppm: 2.24–2.29 (m, 2H, C$\underline{H}_2$), 2.68–2.73 (m, 2H, C$\underline{H}_2$), 3.77 (s, 3H, OC$\underline{H}_3$), 3.82 (s, 3H, OC$\underline{H}_3$), 3.84 (s, 3H, OC$\underline{H}_3$), 6.67 (dd, J = 8.4, 2.1 Hz, 1H, H-5′), 6.73 (d, J = 2.4 Hz, 1H, H-3′), 6.90 (d, J = 2.4 Hz, 1H, H-7), 6.94 (dd, J = 8.4, 2.4 Hz, 1H, H-9), 7.16 (d, J = 8.1 Hz, 1H, H-6′), 8.02 (d, J = 8.7 Hz, 1H, H-10), 12.18 (s, 1H, NH, D_2O exchangeable); ^{13}C NMR (DMSO-d_6, 75 MHz) δ ppm: 23.0 (C5), 27.6 (C6), 55.3 (O$\underline{C}H_3$), 55.3 (O$\underline{C}H_3$), 55.6 (O$\underline{C}H_3$), 98.7 (C3′), 105.4 (C5′), 112.5 (2C), 113.5, 116.4, 116.4, 120.5, 126.9 (2C), 130.0 (2C),

141.6, 156.8 (2C), 160.9, 161.4, 161.6; MS (EI) *m/z* (%): 388.18 (M^+, 13.88), 239.03 (100); Anal. Calcd. for $C_{23}H_{20}N_2O_4$ (388.42): C, 71.12; H, 5.19; N, 7.21; Found C, 71.33; H, 5.21, N, 7.27.

*4.1.8.6. 4-(3,4-Dimethoxyphenyl)-8-methoxy-2-oxo-1,2,5,6-tetrahydrobenzo [h]quinoline-3-carbonitrile (**19c**)*. Yellow crystals in 80% yield, m.p. > 300 °C (reported m.p. > 300 °C) [42]; IR (KBr, ν cm^{-1}): 3450 (NH), 2219 (C≡N), 1632 (C═O); ^{1}H NMR (DMSO-d_6, 400 MHz) δ ppm: 2.51–2.54 (m, 2H, C$\underline{H}_2$), 2.71–2.74 (m, 2H, C$\underline{H}_2$), 3.78 (s, 3H, OC$\underline{H}_3$), 3.83 (s, 3H, OC$\underline{H}_3$), 3.84 (s, 3H, OC$\underline{H}_3$), 6.93–6.97 (m, 3H, H-7, H-9 and H-5′), 7.02 (s, 1H, H-2′), 7.11 (d, J = 8 Hz, 1H, H-6′), 8.02 (d, J = 10.4 Hz, 1H, H-10), 12.49 (s, 1H, NH, D_2O exchangeable); ^{13}C NMR (DMSO-d_6, 75 MHz) δ ppm: 23.4 (C5), 27.7 (C6), 55.3 (O$\underline{C}H_3$), 55.5 (O$\underline{C}H_3$), 55.7 (O$\underline{C}H_3$), 111.7 (2C), 111.9 (2C), 112.5 (2C), 113.4, 116.5, 120.6 (2C), 127.0 (2C), 127.6, 141.6, 148.5, 149.4, 161.5 (2C); MS (EI) *m/z* (%): 388.29 (M^+, 12.38), 311.09 (100); Anal. Calcd. for $C_{23}H_{20}N_2O_4$ (388.42): C, 71.12; H, 5.19; N, 7.21; Found: C, 71.24; H, 5.23; N, 7.34

4.2. Anticancer activity

4.2.1. In vitro cytotoxicity

Cell lines: four tumor cell lines namely; Liver carcinoma cell line (HepG2), Breast carcinoma cell line (MCF-7), Colon carcinoma cell line (HCT116) and Colon carcinoma cell line (Caco-2), and one normal cell line (BHK-21 normal fibroblast) were provided from National Cancer Institute, Cairo University.

SRB Assay: Potential antitumor activity and cytotoxicity of compounds were tested using SRB technique. Tumor cells were plated in 96 multi-well plates (104 cells/well) for 24 h before treatment with compounds to allow attachment of cell to the wall of the plate. Then, different concentrations of each compound at (0, 1, 2.5, 5 and 10 μg/ml) were added to the cell monolayer triplicate wells after being prepared for each individual dose. Monolayer cells were incubated with the compound for 48 h at 37 °C and in atmosphere of 5% CO_2. After 48 h, cells were fixed, washed and stained with Sulforhodamine B stain (SRB). Excess of stain was washed with acetic acid and attached stain was recovered with Tris EDTA buffer. The color intensity was measured in an ELISA reader. The relation between surviving fraction and drug concentration is plotted to get the survival curve of each tumor cell line [43].

4.2.2. In vitro EGFR kinase assay

Compounds **13a**, **13b**, **15a**, **15c**, **17a**, **19b** and **19c** were tested in vitro for inhibition of EGFR tyrosine kinase using ADP-Glo™ Kinase Assay (Promega, Catalogue No. V3831) which is a luminescent kinase assay that measures ADP formed from a kinase reaction. ADP is converted into ATP which is converted into light by Ultra-Glo™ Luciferase. The luminescent signal positively correlates with ADP amount and kinase activity.

Protocol: first dilute enzyme, substrate, ATP and inhibitors in Tyrosine Kinase Buffer (40 mM Tris,7.5; 20 mM $MgCl_2$; 0.1 mg/ml BSA (bovine serum albumin); 2 mM $MnCl_2$; 50 μM DTT), then add to the wells of 384 low volume plate: 1 μl of inhibitor or (5% DMSO), 2 μl of enzyme and 2 μl of substrate/ATP mix. Incubate at room temperature for 60 min, add 5 μl of ADP-Glo™ Reagent, incubate at room temperature for 40 min, add 10 μl of Kinase Detection reagent, incubate at room temperature for 30 min and finally record luminescence (Integration time 0.5–1 s).

4.3. Molecular docking

Molecular Operating Environment (MOE 2014.0901) is the software used for the docking simulation and calculation. All minimizations were performed with MOE until a RMSD gradient of 0.05 kcal mol^{-1} $A^{\circ -1}$ with MMFF94x force field and the partial charges were automatically calculated. The x-ray crystallographic structure of EGFR kinase domain co-crystallized with erlotinib was retrieved from protein data bank https://www.rcsb.org/ (PDB: 1M17). The receptor was prepared for docking study using Protonate 3D protocol in MOE with default options. Docking was done using Triangle Matcher placement method and London dG scoring function, refinement of the results was done using Force field energy and validation process was carried out by redocking the co-crystallized ligand (erlotinib) into EGFR-TK binding site and then its scoring energy (S) and root mean square deviation (rmsd) were calculated. Finally, its interaction with amino acids in the active site was studied. Docking was done using pharmacophore query having 2 features (hydrogen bond with Met769 and a water mediated hydrogen bond with Thr766) [36].

References

[1] B.W. Stewart, C.P. Wild, World Cancer Report 2014, World Heal. Organ., 2014.
[2] Lindsey A. Torre, Freddie Bray, Rebecca L. Siegel, Jacques Ferlay, Joannie Lortet-Tieulent, Ahmedin Jemal, Global cancer statistics, 2012: Global Cancer Statistics, 2012, CA: Cancer J. Clin. 65 (2) (2015) 87–108, https://doi.org/10.3322/caac.21262.
[3] M.L. Rothenberg, D.P. Carbone, D.H. Johnson, Improving the evaluation of new cancer treatments: challenges and opportunities, Nat. Rev. Cancer 3 (4) (2003) 303–309.
[4] C. Avendano, J.C. Menendez, Medicinal Chemistry of Anti- Cancer Drugs, first ed., Elsevier, Amsterdam, 2008.
[5] N.R. Patel, B.S. Pattni, A.H. Abouzeid, V.P. Torchilin, Nanopreparations to overcome multidrug resistance in cancer, Adv. Drug Deliv. Rev. 65 (13–14) (2013) 1748–1762.
[6] P.D.W. Eckford, F.J. Sharom, ABC efflux pump-based resistance to chemotherapy drugs, Chem. Rev. 109 (7) (2009) 2989–3011.
[7] M.C. Brahimi-Horn, J. Chiche, J. Pouysségur, Hypoxia and cancer, J. Mol. Med. 85 (12) (2007) 1301–1307.
[8] M.J. O'Connor, Targeting the DNA damage response in cancer, Mol. Cell 60 (4) (2015) 547–560.
[9] C. Yewale, D. Baradia, I. Vhora, S. Patil, A. Misra, Epidermal growth factor receptor targeting in cancer: a review of trends and strategies, Biomaterials 34 (34) (2013) 8690–8707.
[10] M. Katz, I. Amit, Y. Yarden, Regulation of MAPKs by growth factors and receptor tyrosine kinases, Biochim. Biophys. Acta - Mol. Cell Res. 1773 (8) (2007) 1161–1176.
[11] N. Prenzel, O.M. Fischer, S. Streit, S. Hart, A. Ullrich, The epidermal growth factor receptor family as a central element for cellular signal transduction and diversification, Endocr. Relat. Cancer 8 (1) (2001) 11–31.
[12] R. Roskoski, The ErbB/HER receptor protein-tyrosine kinases and cancer, Biochem. Biophys. Res. Commun. 319 (1) (2004) 1–11.
[13] N. Tebbutt, M.W. Pedersen, T.G. Johns, Targeting the ERBB family in cancer: couples therapy, Nat. Rev. Cancer 13 (9) (2013) 663–673.
[14] J. Zhang, P.L. Yang, N.S. Gray, Targeting cancer with small molecule kinase inhibitors, Nat. Rev. Cancer 9 (1) (2009) 28–39.
[15] H. Masuda, D. Zhang, C. Bartholomeusz, H. Doihara, G.N. Hortobagyi, N.T. Ueno, Role of epidermal growth factor receptor in breast cancer, Breast Cancer Res. Treat. 136 (2) (2012) 331–345.
[16] R. Costa, et al., Targeting epidermal growth factor receptor in triple negative breast cancer: new discoveries and practical insights for drug development, Cancer Treat. Rev. 53 (2017) 111–119.
[17] R.S.M. Ismail, et al., Novel series of 6-(2-substitutedacetamido)-4-anilinoquinazolines as EGFR-ERK signal transduction inhibitors in MCF-7 breast cancer cells, Eur. J. Med. Chem. 155 (Jul. 2018) 782–796.
[18] S. Shagufta, I. Ahmad, An insight into the therapeutic potential of quinazoline derivatives as anticancer agents, Medchemcomm 8 (5) (2017) 871–885.
[19] D. Das, J. Hong, Recent advancements of 4-aminoquinazoline derivatives as kinase inhibitors and their applications in medicinal chemistry, Eur. J. Med. Chem. 170 (2019) 55–72.
[20] R.S.M. Ismail, N.S.M. Ismail, S. Abuserii, D.A. Abou El Ella, Recent advances in 4-aminoquinazoline based scaffold derivatives targeting EGFR kinases as anticancer agents, Futur. J. Pharm. Sci. 2 (1) (2016) 9–19.
[21] A.J. Barker, et al., Studies leading to the identification of ZD1839 (iressa™): an orally active, selective epidermal growth factor receptor tyrosine kinase inhibitor targeted to the treatment of cancer, Bioorg. Med. Chem. Lett. 11 (14) (2001) 1911–1914.
[22] R.T. Dungo, G.M. Keating, Afatinib: first global approval, Drugs 73 (13) (2013) 1503–1515.
[23] Y. Wang, G. Schmid-Bindert, C. Zhou, Erlotinib in the treatment of advanced non-small cell lung cancer: an update for clinicians, Ther. Adv. Med. Oncol. 4 (1) (2012) 19–29.
[24] F. Tan, et al., Icotinib (BPI-2009H), a novel EGFR tyrosine kinase inhibitor, displays potent efficacy in preclinical studies, Lung Cancer 76 (2) (2012) 177–182.
[25] J.E. Frampton, Lapatinib, Drugs 69 (15) (Oct. 2009) 2125–2148.
[26] O. Afzal, et al., A review on anticancer potential of bioactive heterocycle quinoline, Eur. J. Med. Chem. 97 (2015) 871–910.
[27] M.A. Cherian, C.X. Ma, The role of neratinib in HER2-driven breast cancer, Futur.

Oncol. 13 (22) (2017) 1931–1943.
[28] D. Viola, V. Cappagli, R. Elisei, Cabozantinib (XL184) for the treatment of locally advanced or metastatic progressive medullary thyroid cancer, Futur. Oncol. 9 (8) (2013) 1083–1092.
[29] A. Vultur, et al., SKI-606 (bosutinib), a novel Src kinase inhibitor, suppresses migration and invasion of human breast cancer cells, Mol. Cancer Ther. 7 (5) (2008) 1185–1194.
[30] J. Matsui, Y. Funahashi, T. Uenaka, T. Watanabe, A. Tsuruoka, M. Asada, Multi-kinase inhibitor E7080 suppresses lymph node and lung metastases of human mammary breast tumor MDA-MB-231 via inhibition of vascular endothelial growth factor-receptor (VEGF-R) 2 and VEGF-R3 kinase, Clin. Cancer Res. 14 (17) (2008) 5459–5465.
[31] J.S. Park, K.A. Yu, T.H. Kang, S. Kim, Y.-G. Suh, Discovery of novel indazole-linked triazoles as antifungal agents, Bioorg. Med. Chem. Lett. 17 (12) (2007) 3486–3490.
[32] K.P. Harish, K.N. Mohana, L. Mallesha, Synthesis of indazole substituted-1,3,4-thiadiazoles and their anticonvulsant activity, Drug Invent. Today 5 (2) (Jun. 2013) 92–99.
[33] A. Upadhyay, S.K. Srivastava, S.D. Srivastava, Conventional and microwave assisted synthesis of Some new N-[(4-oxo-2-substituted aryl −1, 3-thiazolidine)-acetamidyl]-5-nitroindazoles and its antimicrobial activity, Eur. J. Med. Chem. 45 (9) (2010) 3541–3548.
[34] J. Dong, Q. Zhang, Z. Wang, G. Huang, S. Li, Recent advances in the development of indazole-based anticancer agents, ChemMedChem 13 (15) (2018) 1490–1507.
[35] F.A.B. Schutz, T.K. Choueiri, C.N. Sternberg, Pazopanib: clinical development of a potent anti-angiogenic drug, Crit. Rev. Oncol. Hematol. 77 (3) (2011) 163–171.
[36] J. Stamos, M.X. Sliwkowski, C. Eigenbrot, Structure of the epidermal growth factor receptor kinase domain alone and in complex with a 4-anilinoquinazoline inhibitor, J. Biol. Chem. 277 (48) (2002) 46265–46272.
[37] N. Minami, Y. Suzuki, Synthesis of naphthisoxazole derivatives. I. Synthesis of 4,5-dihydronaphth(2,1-d)isoxazole derivatives (author's transl), Yakugaku Zasshi 95 (7) (1975) 815–821.
[38] K.W. Bentley, W.C. Firth, The synthesis of potential androgens Part II, J. Chem. Soc. (1955) 2403–2408.
[39] H. Wünscher, G. Haucke, P. Czerney, U. Kurzer, Photochromic properties of hydrolyzed benzopyrylium salts—the influence of substituents, J. Photochem. Photobiol. A Chem. 151 (1–3) (2002) 75–82.
[40] Y. Gautam, et al., 2-(3′,4′-Dimethoxybenzylidene)tetralone induces anti-breast cancer activity through microtubule stabilization and activation of reactive oxygen species, RSC Adv. 6 (40) (2016) 33369–33379.
[41] B. Janardhan, S.V. Laxmi, B. Rajitha, One-pot synthesis of fused 3,4-dihydropyrimidin-2(1H)-ones and thiones using a novel ionic liquid as an efficient and reusable catalyst: improved protocol conditions for the Biginelli-like scaffolds, Heterocycl. Commun. 18 (2) (2012) 93–97.
[42] M. Ebied, W. Zaghary, K. Amin, S. Hammad, Synthesis and antimicrobial evaluation of some tricyclic substituted benzo[h]quinazolines, benzo[h]quinolines and naphthaleno[d]thiazoles, J. Adv. Pharm. Res. 1 (4) (2017) 216–227.
[43] P. Skehan, et al., New colorimetric cytotoxicity assay for anticancer-drug screening, JNCI J. Natl. Cancer Inst. 82 (13) (1990) 1107–1112.